The following supplement accompanies the article

Scale-dependent detection of the effects of harvesting a marine fish population

Valerio Bartolino[1,2,*], Lorenzo Ciannelli[3], Paul Spencer[4], Thomas K. Wilderbuer[4], Kung-Sik Chan[5]

[1]Marine Research Institute, Department of Aquatic Resources, Swedish University of Agricultural Sciences, Lysekil 45321, Sweden

[2]Regional Climate Group, Department of Earth Sciences, University of Gothenburg, 40530 Gothenburg, Sweden
[3]College of Oceanic and Atmospheric Sciences, Oregon State University, Corvallis, Oregon 97331, USA
[4]Alaska Fisheries Science Center, NOAA, Seattle, Washington 98115, USA
[5]Department of Statistics and Actuarial Science, University of Iowa, Iowa City, Iowa 52242, USA

*Email: valerio.bartolino@slu.se

Marine Ecology Progress Series: 444: 251–261 (2012)

Supplement 1. Standardized annual indices of abundance of yellowfin sole in the eastern Bering Sea (Fig. S1)

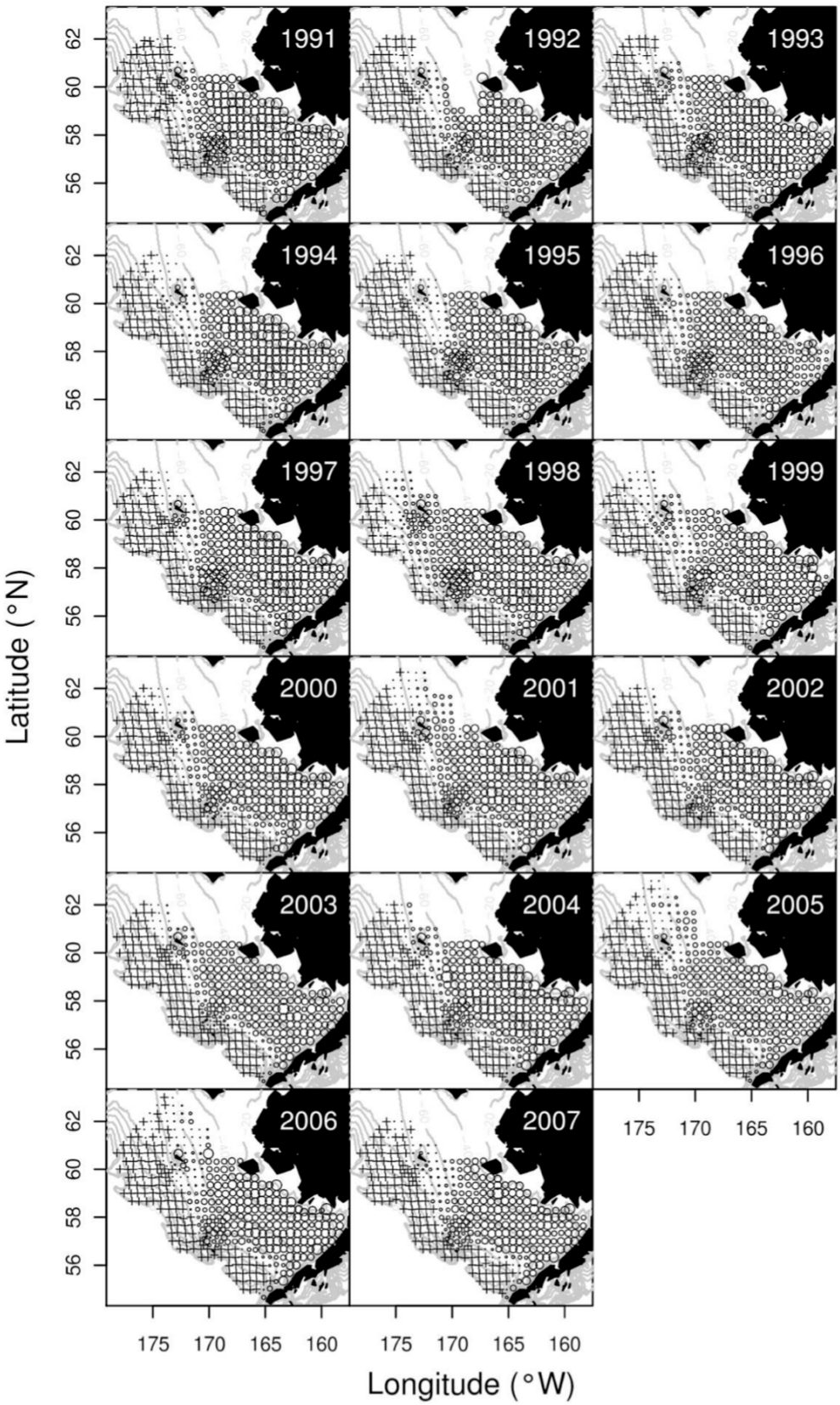

Fig. S1. Yellow fin sole densities in the eastern Bering Sea as estimated from the groundfish survey data collected by the US National Marine Fisheries Service during 1991–2007. The sampling design is based on a fixed regular grid of 37 x 37 km, and a finer sampling grid of 18.5 x 18.5 km around the Pribilof Islands. Circle size is proportional to the log-transformed local density of fish ln(kg km^{-2}), and crosses indicate zero hauls

Supplement 2. Weighted catch variable

Our intent was to investigate the scale at which harvest affects abundance. To this extent we used a statistical model that contained a harvest effect at a variety of scales, and then estimated the scale at which the model best reproduced the observed data. Specifically, we fixed in the model a large-scale harvest effect representative of regional depletion, and then we added an additional harvest term at progressively smaller scales. We opted to fix the large-scale effect because this species has a long and documented history of commercial exploitation, and has in the past been overfished (Wilderbuer et al. 2008). In this section we explain how the temporal and spatial scales of harvest were calculated.

Catches occurring within a short time before the survey sample were weighted higher than catches farther back in time, and catches closer in space were weighted higher than those taking place farther away. We assumed that the movement of fish, which ultimately spreads and constrains the effect of catch, follows an isotropic diffusion process. Consequently weighting was accomplished using a Gaussian kernel on both time and space:

$$w(z) = e^{-(z^2)/(2\sigma^2)} \qquad \text{(S1)}$$

where z is either time measured in day of year or space measured in km. Small values of σ define a sharp decrease, while large values of σ signify a more gradual decrease of the weight curve. Finally, the predictor variable representing the intensity of harvesting C associated to each survey point at geographical coordinates ρ,λ, day t and year y, was calculated as the sum of the weighted catches that occurred before the survey:

$$C_{t,y,(\rho,\lambda)} = \sum_{i=1}^{n} w_{1i} w_{2i} C_i \qquad \text{(S2)}$$

where w_{1i} and w_{2i} are the temporal and spatial weights of the commercial catch C_i occurring during the previous 12 mo, as derived from Eq. (1). The effect of fisheries harvesting was explored at a variety of spatial and temporal scales by varying the value of σ in the weighting scheme. We assumed a fixed large scale harvest term using a σ that corresponded to a weight value of approximately 0.6 for catches occurring 290 d apart and 900 km apart (Fig. S2). Given the relative large value of σ, the large-scale catches are rather homogeneous throughout the study area, and represent the regional effect of harvesting. For the smaller scale, we explored the model goodness of fit over a wide range of scales (see 'Multiscale analysis' in main article).

LITERATURE CITED

Wilderbuer TK, Nichol DG, Ianelli J (2008) Yellowfin sole, North Pacific Fishery Management Council. In: NPFMC Bering Sea and Aleutian Islands, SAFE Rep, Anchorage, AK

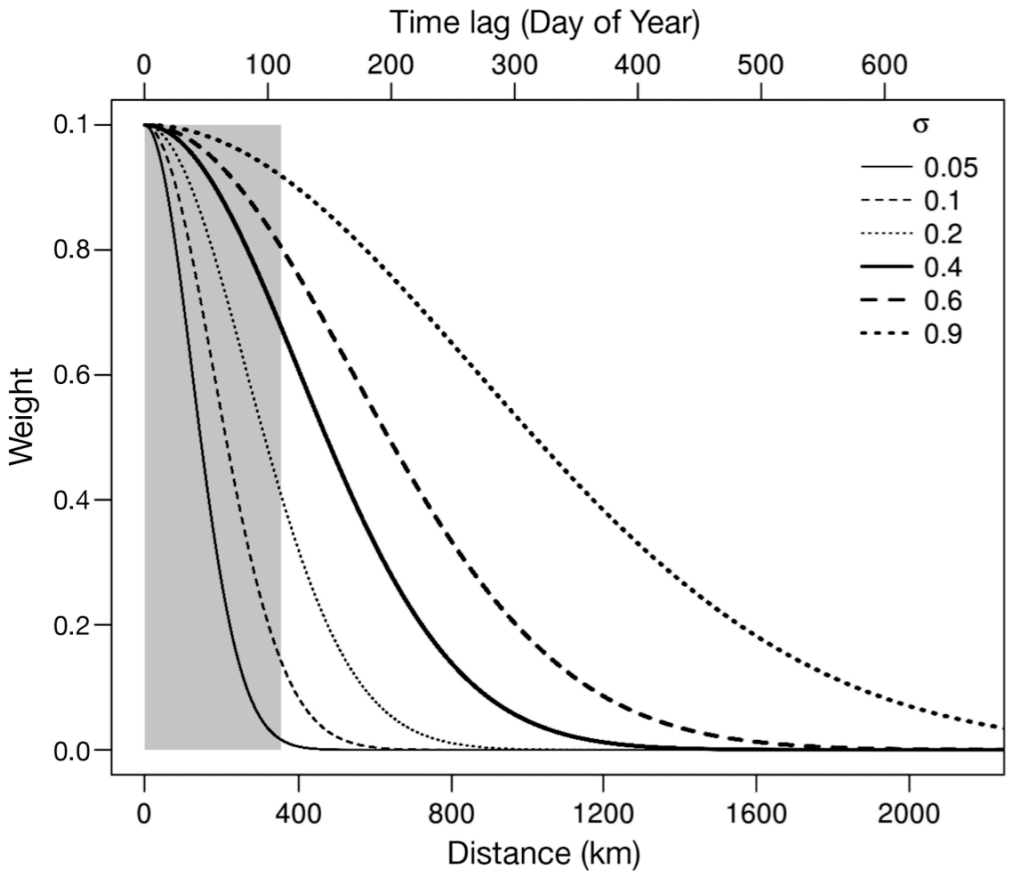

Fig. S2. Gaussian kernel weight curves. The shaded area represents the scale of aggregation of yellowfin sole calculated as the maximum distance where yellowfin sole densities are auto-correlated in space (range parameter σ from Gaussian variogram model)

Supplement 3. **Mixed effect model**

Spatial autocorrelation can affect model estimates in 2 main ways: overestimating the significance level of the model covariates, and potentially affecting smoothing estimation with the risk of incorrect interpretation of some of the covariate effects (Agostini et al. 2008, Ciannelli et al. 2008). To produce unbiased estimates of covariate p-values and to verify that the presence of a spatial correlation did not affect covariate effects (Fig. A3), we used a mixed model approach. For this purpose, a generalized additive mixed model (GAMM) was built as extension of the spatially variable coefficient model for commercial trawler CPUEs. GAMMs allow to include spatially autocorrelated within-group errors (Venables & Ripley 2002, Dormann et al. 2007) that can then be treated as a random effect (Pinheiro & Bates 2000). The regression model was formulated as follows:

$$\mathrm{CPUE}_{t,y,(\phi,\lambda)} = a_y + g_1(t) + \begin{cases} s_1(\rho,\lambda) + \alpha_1 \cdot C'_{t,y,(\rho,\lambda)} + s_2(\rho,\lambda) \cdot C'_{t,y,(\rho,\lambda)} + \gamma_{1y,(\rho,\lambda)} + e_{t,y,(\rho,\lambda)} & \text{Period 1} \\ s_3(\rho,\lambda) + \alpha_2 \cdot C'_{t,y,(\rho,\lambda)} + s_4(\rho,\lambda) \cdot C'_{t,y,(\rho,\lambda)} + \gamma_{2y,(\rho,\lambda)} + e_{t,y,(\rho,\lambda)} & \text{Period 2} \\ s_5(\rho,\lambda) + \alpha_3 \cdot C'_{t,y,(\rho,\lambda)} + s_6(\rho,\lambda) \cdot C'_{t,y,(\rho,\lambda)} + \gamma_{3y,(\rho,\lambda)} + e_{t,y,(\rho,\lambda)} & \text{Period 3} \\ s_7(\rho,\lambda) + \alpha_4 \cdot C'_{t,y,(\rho,\lambda)} + s_8(\rho,\lambda) \cdot C'_{t,y,(\rho,\lambda)} + \gamma_{4y,(\rho,\lambda)} + e_{t,y,(\rho,\lambda)} & \text{Period 4} \end{cases} \quad \text{(S3)}$$

The deterministic part of the model (parametric coefficients α and smoothing functions *s* relating the predictors to the response variable) was equivalent to that presented in model 5 (Table 1). The error part of the model was separated into a spatially autocorrelated random component described by a Gaussian correlation structure (γ) calculated by year and fishing period, and a normally distributed error term (*e*). Due to computational limits the model was fitted on a subsample (10%) of the original dataset. For ensuring representativeness, 10% of the dataset was randomly sampled maintaining the original proportion of observations for each year and fishing period.

LITERATURE CITED

Agostini VN, Hendrix AN, Hollowed AB, Wilson CD, Pierce SD, Francis RC (2008) Climate-ocean variability and pacific hake: A geostatistical modelling approach. J Mar Syst 71:237–248

Ciannelli L, Fauchald P, Chan KS, Agostini VN, Dingsor GE (2008) Spatial fisheries ecology: recent progress and future prospects. J Mar Syst 71:223–236

Dormann CF, McPherson JM, Araujo MB, Bivand R and others (2007) Methods to account for spatial autocorrelation in the analysis of species distributional data: a review. Ecography 30:609–628

Pinheiro JC, Bates DM (2000) Mixed-Effects Models in S and S-PLUS. Springer, New York, NY

Venables WN, Ripley BD (2002) Modern Applied Statistics with S. Springer, New York, NY

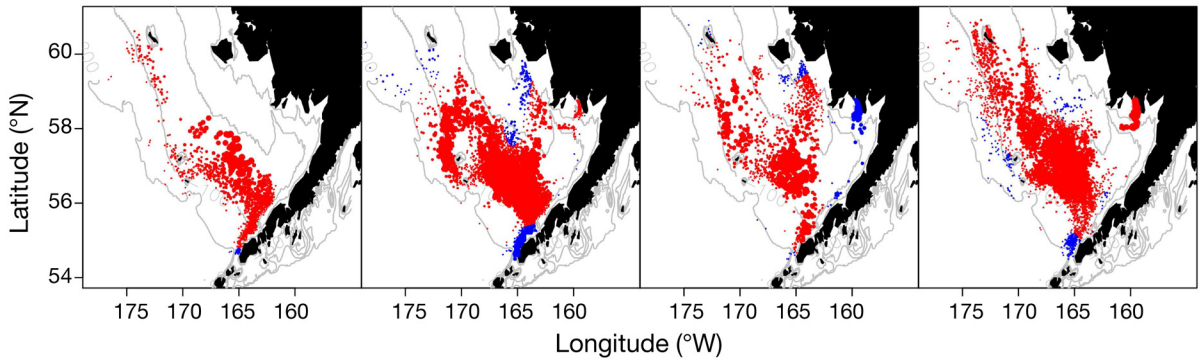

Fig. S3. Effects of log-transformed fisheries catch at small scale on yellowfin sole abundance (CPUE) during the 4 main fishing seasons (left–right: December–January, February–May, June–July, and August–November) as estimated from generalized additive mixed model. Red and blue bubbles indicate a positive and a negative effect, respectively

Supplement 4. Main effects from the invariant coefficient model (Fig. S4)

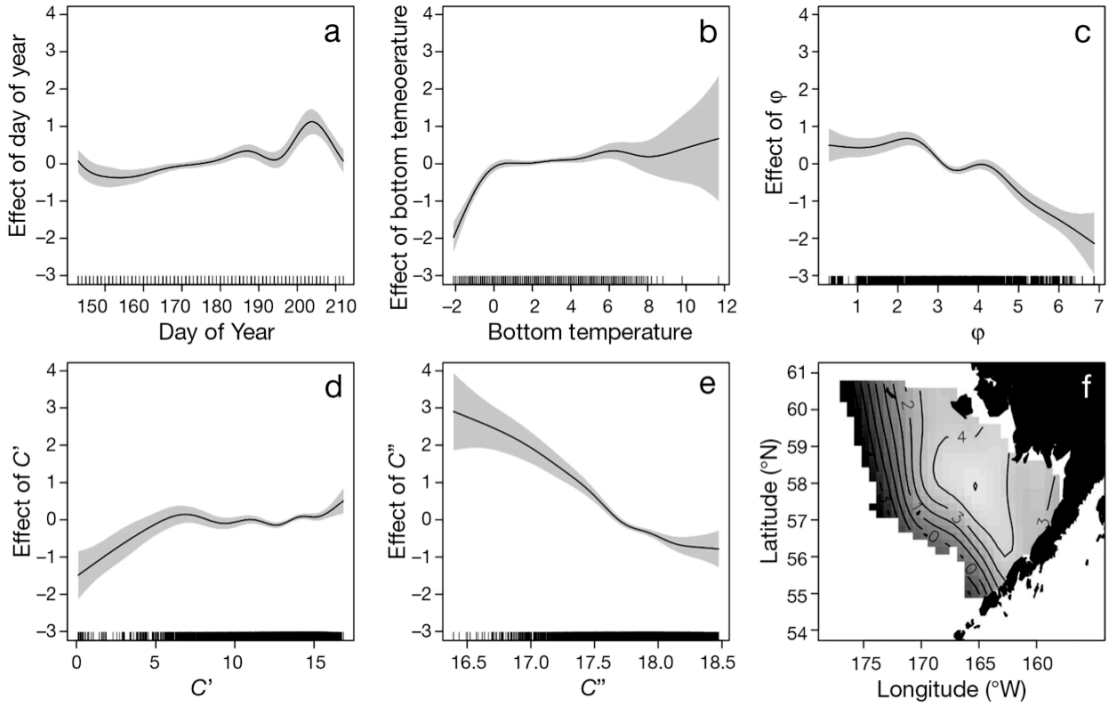

Fig. S4. Effects of (a) day of year, (b) bottom temperature, (c) sediment size, (d) small-scale and (e) large-scale log-transformed fisheries catch, and (f) geographical position on yellowfin sole local density as estimated from the spatially invariant formulation (Model 1 in Table 1), with the shaded regions indicating 95% confidence interval. Ticks along *x*-axis indicate measurement points